



The inhibition of TRPML1/TFEB leads to lysosomal biogenesis disorder, contributes to developmental fluoride neurotoxicity

Jingjing Zhang^{a,b,c,d}, Yanling Tang^{a,b,c,d}, Zeyu Hu^{a,b,c,d}, Wanjing Xu^{a,b,c,d}, Yue Ma^{a,b,c,d}, Panpan Xu^{a,b,c,d}, Hengrui Xing^{a,b,c,d}, Qiang Niu^{a,b,c,d,*}

^a Department of Preventive Medicine, School of Medicine, Shihezi University, Shihezi, Xinjiang, People's Republic of China

^b Key Laboratory of Preventive Medicine, Shihezi University, Shihezi, Xinjiang, People's Republic of China

^c Key Laboratory of Xinjiang Endemic and Ethnic Diseases (Ministry of Education), School of Medicine, Shihezi University, Shihezi, Xinjiang, People's Republic of China

^d NHC Key Laboratory of Prevention and Treatment of Central Asia High Incidence Diseases, First Affiliated Hospital, School of Medicine, Shihezi University, People's Republic of China

ARTICLE INFO

Edited by Dr Hyo-Bang Moon

Keywords:

Fluoride
Developmental neurotoxicity
Lysosomal biogenesis
TRPML1/TFEB
Pyroptosis

ABSTRACT

Fluoride is capable of inducing developmental neurotoxicity; regrettably, the mechanism is obscure. We aimed to probe the role of lysosomal biogenesis disorder in developmental fluoride neurotoxicity—specifically, the regulating effect of the transient receptor potential mucolipin 1 (TRPML1)/transcription factor EB (TFEB) signaling pathway on lysosomal biogenesis. Sprague-Dawley rats were given fluoridated water freely, during pregnancy to the parental rats to 2 months after delivery to the offspring. In addition, neuroblastoma SH-SY5Y cells were treated with sodium fluoride (NaF), with or without mucolipin synthetic agonist 1 (ML-SA1) or adenovirus TFEB (Ad-TFEB) intervention. Our findings revealed that NaF impaired learning and memory as well as memory retention capacities in rat offspring, induced lysosomal biogenesis disorder, and decreased lysosomal degradation capacity, autophagosome accumulation, autophagic flux blockade, apoptosis, and pyroptosis. These changes were evidenced by the decreased expression of TRPML1, nuclear TFEB, LAMP2, CTSB, and CTSD, as well as increased expression of LC3-II, p62, cleaved PARP, NLRP3, Caspase1, and IL-1 β . Furthermore, TRPML1 activation and TFEB overexpression both restored TFEB nuclear protein expression and promoted lysosomal biogenesis while enhancing lysosomal degradation capacity, recovering autophagic flux, and attenuating NaF-induced apoptosis and pyroptosis. Taken together, these results show that NaF promotes the progression of developmental fluoride neurotoxicity by inhibiting TRPML1/TFEB expression and impeding lysosomal biogenesis. Notably, the activation of TRPML1/TFEB alleviated NaF-induced developmental neurotoxicity. Therefore, TRPML1/TFEB may be promising markers of developmental fluoride neurotoxicity.

1. Introduction

The element fluorine is widespread in the natural environment of the Earth. Water, food, and air can all contribute to its entry into the body. Industrial emissions, pesticide residues, and household chemical products, such as toothpaste, are also important sources of fluoride (Caldas et al., 2022; Wang et al., 2019). Moderate fluoride intake is beneficial for preventing dental caries and strengthening bones. Nevertheless,

long-term exposure to superabundant fluoride causes not only skeletal system fluorosis, with dental and skeletal fluorosis as the primary manifestations, but also adverse effects on other non-skeletal systems (Zhou et al., 2022a). Given that drinking water is one of the main sources of fluoride in humans, the World Health Organization stipulates that the permissible limit of fluoride is 1.5 mg/L in drinking water (Anon, 2022). Due to the nonrenewable nature of neurons, fluoride exposure is particularly harmful to the nervous system (Dec et al., 2017).

Abbreviations: Ad-TFEB, adenovirus TFEB; CTSB, cathepsin B; CTSD, cathepsin D; Caspase1, cysteinyl aspartate specific proteinase 1; IL-1 β , interleukin-1 β ; IQ, intelligence quotient; LAMP2, lysosomal-associated membrane protein 2; LC3, microtubule-associated protein 1 light chain 3; ML-SA1, mucolipin synthetic agonist 1; MOI, multiplicity of infection; NaF, sodium fluoride; NLRP3, NOD-like receptor protein 3; PARP, poly (ADP-ribose) polymerase; SQSTM1/p62, sequestosome 1; TFEB, transcription factor EB; TRPML1, transient receptor potential mucolipin 1.

* Correspondence to: Department of Preventive Medicine, School of Medicine, Shihezi University, North 2th Road, Shihezi, Xinjiang 832000, People's Republic of China.

E-mail address: niuqiang1022@163.com (Q. Niu).

<https://doi.org/10.1016/j.ecoenv.2023.114511>

Received 24 October 2022; Received in revised form 29 December 2022; Accepted 3 January 2023

0147-6513/© 2023 Published by Elsevier Inc. This is an open access article under the CC BY-NC-ND license (<http://creativecommons.org/licenses/by-nc-nd/4.0/>).

Prenatal exposure to adverse factors is extremely hazardous to the development of the brain since the nervous system has not completely matured (De Asis-Cruz et al., 2022). Previous literature indicates that fluoride can accumulate in the fetal brain by crossing the placental and blood-brain barriers in the perinatal stage, causing non-reversible injury to the nervous system, which is more harmful than in adults (Abduweli et al., 2020; Castiblanco-Rubio and Martinez-Mier, 2022). Epidemiological investigations have shown that maternal exposure to fluoride during pregnancy is connected with an inferior intelligence quotient (IQ) in their offspring (Goodman et al., 2022; Green et al., 2019). A cross-sectional study has demonstrated that excessive fluoride exposure can cause cognitive dysfunction in children (Prabhakar et al., 2021). Animal research has demonstrated that fluoride exposure during pregnancy and lactation causes cognitive and motor dysfunction in rats (Ferreira et al., 2021; Souza-Monteiro et al., 2022). Thus, it is apparent from these results that excessive fluoride exposure during early development can lead to severe neurotoxicity (Grandjean, 2019). However, there remains a lack of clarity regarding the specific mechanisms of developmental fluoride neurotoxicity.

Currently, compelling evidence suggests that the mechanisms of fluoride-induced nervous system damage include neurotransmitter release disorders, glial activation, reactive oxygen species production, mitochondrial dysfunction, inflammation, and cell apoptosis (Adkins and Brunst, 2021; Dec et al., 2017; Nagendra et al., 2021). As the centers of material and energy metabolism, mitochondria are involved in the occurrence and development of many neurodegenerative diseases (Coelho et al., 2022). Excessive fluoride intake can destroy the ultrastructure of mitochondria; change mitochondrial permeability; inhibit the mitochondrial respiratory chain; reduce mitochondrial activity, adenosine triphosphate (ATP) content and mitochondrial membrane potential; promote the release of cytochrome C; and lead to cell apoptosis (Wei et al., 2022). Damaged mitochondria are degraded in lysosomes through autophagy and thus, prevented from damaging the nerve cells (Lou et al., 2020).

Neurons are nonrenewable cells. Therefore, the removal of harmful substances from neurons through autophagy is crucial for maintaining intracellular homeostasis (Mizushima and Levine, 2020). Autophagy is crucial for maintaining cellular activity and intracellular homeostasis by forming autophagosomes that transport defective organelles, misfolded and aggregated proteins, and pathogens to lysosomes for degradation and recirculation (Xia et al., 2021). The autophagic dynamic process is called autophagic flux and includes autophagosomal formation and maturation, autophagosome-lysosome fusion, and autophagic substrate degradation in lysosomes. Autophagic flux blockade leads to the aggregation of defective organelles and pathogenic proteins, disrupting intracellular homeostasis and causing neuronal damage, which results in various neurodegenerative diseases (Zhao et al., 2021). Excessive fluoride can inhibit mitochondrial fission and induce mitochondrial abnormalities, resulting in autophagic flux blockade and apoptosis (Zhao et al., 2019). Fluoride exposure has been found to cause autophagosome accumulation and inhibit autophagosome-lysosome fusion, causing autophagic flux blockade, thereby contributing to developmental neurotoxicity (Zhang et al., 2021b). Despite the evidence suggesting a potential connection between autophagic flux blockade and developmental fluoride neurotoxicity, the detailed mechanisms underlying this toxicity are unclear.

Lysosomes are the final components of autophagic flux, containing more than 60 acidic hydrolases that degrade various substrates such as proteins, lipids, senescent organelles, and inactivated cells in autophagosomes and providing raw materials for new biomolecules. They are the cellular processing and recycling systems (Ballabio and Bonifacino, 2020). Lysosomal biogenesis, an essential prerequisite for maintaining normal lysosomal function, involves the following steps. The plasma membrane and posterior Golgi form early endosomes, which experience multiple rounds of fusion and proliferation and gradually mature into late endosomes, eventually forming lysosomes (Mullins and Bonifacino,

2001). Thus, in the case of lysosomal biogenesis disorders, there are insufficient lysosomes available to participate in substrate degradation, resulting in decreased lysosomal degradation capacity and consequent substrate accumulation, leading to lysosomal storage disease and impairment of neuronal function (Rebiai et al., 2021). The transcription factor EB (TFEB) is a central regulator of the lysosomes, which boosts the gene expression required for lysosomal biogenesis and function (Bajaj et al., 2019). TFEB is typically situated in the cytoplasm of the cell. Nevertheless, after exposure to stressful conditions such as starvation, TFEB enters the nucleus, promotes the transcription of lysosome-related genes, facilitates lysosomal biogenesis, and restores normal lysosomal function (Martini-Stoica et al., 2016). Thus, TFEB has evolved into a therapeutic target for various diseases caused by lysosomal biogenesis and dysfunction (Chen et al., 2021). Lysosomal biogenesis requires TFEB nuclear translocation, which is regulated by Ca^{2+} , and the release of Ca^{2+} is controlled by transient receptor potential mucolipin 1 (TRPML1). Upon activation of TRPML1 channels, Ca^{2+} is released from the lysosomal lumen and activates calcineurin to dephosphorylate TFEB, which promotes TFEB nuclear translocation and subsequent lysosomal biogenesis (Ballabio and Bonifacino, 2020). Growing evidence suggests that lysosomal biogenesis disorders and dysfunction are vital causes of autophagic flux blockade in neurons (Gu et al., 2019; Li et al., 2020). However, the effect of lysosomal biogenesis disorder on developmental fluoride neurotoxicity, particularly the effect of TRPML1/TFEB, requires further exploration.

Hence, in the current study, Sprague-Dawley (SD) rats were given fluoridated water freely, from pregnancy to the parental rats to 2 months after delivery to the offspring (to simulate human fluoride exposure during a pivotal stage of neurodevelopment). Human neuroblastoma SH-SY5Y cells were treated with sodium fluoride (NaF), with or without mucolipin synthetic agonist 1 (ML-SA1)—a TRPML1 channel agonist that promotes lysosomal Ca^{2+} release, activates calcineurin, and triggers TFEB nuclear translocation and subsequent lysosomal biogenesis (Kim et al., 2021)—or adenovirus TFEB (Ad-TFEB) intervention. Thus, we aimed to investigate the role of lysosomal biogenesis disorder in developmental fluoride neurotoxicity and establish the scientific and theoretical bases for the treatment and prevention of fluorosis.

2. Materials and methods

2.1. Antibodies, reagents, and chemicals

NaF (7681-49-4) and ML-SA1 (332382-54-4) were obtained from Sigma (USA). mRFP-GFP-LC3 adenoviral vectors were obtained from Hanbio Biotechnology Co., Ltd. (China). Fluo-3 AM was provided by APEX BIO (C5092, USA). LysoTracker Red was supplied by Solarbio Science and Technology Co., Ltd. (L8010, China). The TRPML1 antibody was provided by Thermo Fisher (PA1-46474, USA). Poly (ADP-ribose) polymerase (PARP) (13371-1-AP), cathepsin D (CTSD) (66534-1-Ig), microtubule-associated protein 1 light chain 3 (LC3) (14600-1-AP), glyceraldehyde-3-phosphate dehydrogenase (GAPDH) (10494-1-AP), sequestosome 1 (SQSTM1/p62) (18420-1-AP), TFEB (13372-1-AP), and lysosomal-associated membrane protein 2 (LAMP2) (27823-1-AP) antibodies were provided by Proteintech (USA). Recombinant adenovirus plasmid expressing TFEB was purchased from WZ Biosciences Inc. (China). Cathepsin B (CTSB) (ab214428) and cysteinyl aspartate specific proteinase 1 (Caspase1) (ab179515) antibodies were obtained from Abcam (USA). Interleukin-1 β (IL-1 β) (A00101) and proliferating cell nuclear antigen (PCNA) (BM0104) antibodies and the nuclear protein extraction kit (AR0106) were obtained from Boster Co., Ltd. (China). The NOD-like receptor protein 3 (NLRP3) antibody was purchased from Bioss (bs-10021R, China). Horseradish peroxidase (HRP)-conjugated goat anti-rabbit IgG (ZB-2301), HRP-conjugated goat anti-mouse IgG (ZB-2305), and fluorescein isothiocyanate (FITC)-conjugated goat anti-rabbit IgG (ZF-0311) were purchased from ZSGB-BIO (China).

2.2. Animals and treatments

The Experimental Animal Center of Xinjiang Medical University supplied specific pathogen free (SPF)-rated adult SD rats. The research protocol was approved by the Ethics Committee for Animal Research of the School of Medicine, Shihezi University. The animals were placed in a room with a temperature of 20–25 °C, a humidity of 50–60 %, and a 12 h light-dark cycle. The rats were fed ad libitum with tap water and standardized granular food.

After a week of acclimation, 24 SD rats—8 males and 16 females—were stochastically separated into one control group (tap water with fluoride ion content below 1 mg/L) and three NaF-treatment groups. Rodents remove fluoride from their bodies more efficiently than humans (Angmar-Mansson and Whitford, 1984). Based on prior studies on fluoride neurotoxicity and environmental fluoride levels in drinking water (Zhang, 2021b; Zhao, 2020), we set the NaF dosages to 25, 50, and 100 mg/L (corresponding to 11.3, 22.6, and 45.2 mg/L fluoride ions, respectively). The rats were administered fluoride via drinking water freely to practically simulate real human fluoride exposure as far as possible. Each group contained 6 rats—2 males and 4 females. The rats were kept in cages and mated. After vaginal plug formation, the females were placed in individual cages separately. NaF was given to the pregnant female rats from pregnancy to 21 days postpartum. The rat offspring received NaF through maternal breastfeeding during the lactation period of 21 days. After that, 6 offspring were stochastically chosen from each group; the male-to-female ratio was 1:1. After the weaning period, the offspring received the identical treatments as the maternal rats until postnatal days (PND) 60. Two months later, the animals were euthanized within 8 h, and the hippocampus was promptly separated, wrapped in tinfoil, placed in autoclaved Eppendorf tubes, immersed in liquid nitrogen for 10 s, and then transferred to –80 °C for storage.

2.3. Cell culture and treatment

The American Type Culture Collection (USA) provided SH-SY5Y cells. Cells were cultured in Dulbecco's modified Eagle's medium (DMEM) with fetal bovine serum (FBS) (10 %), streptomycin (100 mg/ML), and penicillin (100 U/ML) in a humidified environment (37 °C, 5 % CO₂). When the cell density reached 85 % in the culture vessel, 0, 20, 40, or 60 mg/L of NaF (corresponding to 9.04, 18.08, or 27.12 mg/L fluoride ions, respectively) was added and incubated for 24 h (the dosages in the current study were based on prior research (Zhang et al., 2021b; Zhao et al., 2020)). ML-SA1 powder was dissolved in dimethyl sulfoxide to produce a stock solution with a concentration of 20 mmol/L and then diluted to 10 μmol/L with medium before addition to the cells. The cells were treated with ML-SA1 for 1 h before being treated with 60 mg/L NaF for 24 h. In parallel, the cells were transfected with a control adenovirus (Ad-null) or a recombinant adenovirus plasmid expressing TFEB (multiplicity of infection (MOI) = 400). After 24 h of incubation with Ad-TFEB or Ad-null, 60 mg/L NaF was added to the cells for another 24 h.

2.4. Morris water maze (MWM) test

The water was blackened by mixing it with non-toxic ink to keep the platform hidden in the MWM test. In the place navigation test (PNT), for the first four consecutive days, each offspring was allowed to find the hidden platform for a maximum of 60 s. If the rats reached the platform within 60 s, the escape latency was documented; if not, the rat's escape latency was documented as 60 s. The escape latency, swimming route, distance, and speed were documented to assess the rat's learning and memory capacities. In the space probe test (SPT), the rat was monitored while swimming freely for 60 s after removing the platform. The time spent in the target quadrant, the number of platform crossings, the distance covered in the target quadrant, and the swimming route were

documented to assess the memory retention capacity of rats.

2.5. Western blot

The concentrations of proteins extracted from SH-SY5Y cells or hippocampi were measured using BCA protein assay kits. Proteins were resolved by sodium dodecyl sulfate–polyacrylamide gel electrophoresis and blotted onto polyvinylidene fluoride (PVDF) membranes. Next, the membranes were blocked with 5 % non-fat milk for at least 1 h, followed by incubation with primary antibodies for 16–18 h at 4 °C (TRPML1 (1:2000), TFEB (1:1000), LC3 (1:1000), p62 (1:1000), Caspase1 (1:1000), IL-1β (1:1000), LAMP2 (1:1000), CTSB (1:1000), NLRP3 (1:1000), CTSD (1:1000), PARP (1:1000), GAPDH (1:1000), or PCNA (1:1000)). Subsequently, the membranes were incubated with secondary antibodies (1:20,000) for 2 h at room temperature. The protein bands were visualized using enhanced chemiluminescence (ECL) reagents and the band intensities were quantified using ImageJ software. The experiments were performed three times independently.

2.6. Autophagic flux detection

Autophagic flux was monitored using mRFP-GFP-LC3 adenoviral vectors. When the SH-SY5Y cells grew to 30–50 % in the 24-well plate, mRFP-GFP-LC3 adenovirus (MOI = 400) was added to infect the cells for 16 h at 37 °C, followed by another 24 h of culture with 0, 20, 40, or 60 mg/L NaF. A fluorescence microscope (Japan) was used for analyzing the mRFP-GFP-LC3 distribution, and ImageJ software was used to quantify the distribution.

2.7. Immunofluorescence

SH-SY5Y cells were cultured in a 24-well plate. After the indicated treatments, the cells underwent fixation, permeabilization, and sealing processes. Next, the cells were incubated overnight with the TFEB (1:100) primary antibody at 4 °C. Next, the cells were incubated with the FITC-conjugated goat anti-rabbit IgG secondary antibody (1:50) for 1 h. After being stained with DAPI, the fluorescence intensity of the cells was observed using a fluorescence microscope (Japan). Quantification was done using ImageJ.

2.8. Lysosome detection

Lyso-Tracker Red stock solution was diluted to 50 nM with medium at a ratio of 1:20,000 to detect lysosomes. When the SH-SY5Y cells grew to 70 % in the 48-well plate, 0, 20, 40, or 60 mg/L of NaF was added to the cells for 24 h at 37 °C. Then, the cells were treated with diluted LysoTracker Red for 2 h. The fluorescence intensity of the cells was observed by using a fluorescence microscope (Japan). Experiments were performed three times independently.

2.9. Ca²⁺ detection

A Fluo-3 AM stock solution was diluted to 5 μM with medium (without FBS) to detect Ca²⁺. When the cells grew to 70 % in the 48-well plate, 0, 20, 40, or 60 mg/L of NaF were added to the cells for 24 h at 37 °C. Then, the cells were cultured with diluted Fluo-3 AM for 1 h. The fluorescence intensity of the cells was observed by using a fluorescence microscope (Japan). Experiments were performed three times independently.

2.10. Transmission electron microscopy (TEM)

Three rat hippocampal samples were randomly chosen from each group to observe the ultrastructure. The samples were cut into 1 mm³ blocks and fixed with 2.5 % precooled glutaraldehyde for 6 h at 4 °C. Then, the blocks were dehydrated with ethanol and acetone, infiltrated

with a mixture of one-half propylene oxide and embedded in resin. Next, 50 nm-thick sections were cut and stained with 4 % uranyl acetate for 25 min and 0.5 % lead citrate for 10 min. The ultrastructure of the hippocampal region was observed under a TEM (Philips Tecnai10, Holland).

2.11. Statistical analysis

SPSS 26.0 software was used to analyze the data. All the data were expressed as the mean \pm standard deviation (SD). One-way ANOVA, followed by the Tukey test, was used for multiple comparisons. $P < 0.05$ was considered statistically significant.

3. Results

3.1. NaF exposure impairs learning and memory as well as memory retention capacities in offspring rats

In the PNT, the swimming speed of offspring rats was observably diminished in the group treated with NaF on the second day ($P < 0.05$; Fig. 1 A). The escape latency of the group treated with NaF on the second day was observably longer ($P < 0.05$; Fig. 1B). The swimming distance in NaF treatment group was remarkably longer on the first day ($P < 0.05$; Fig. 1C). In the SPT, the platform crossing number of offspring rats was notably diminished after NaF exposure ($P < 0.05$; Fig. 1E). The time and distance of the target quadrants of the offspring rats treated with NaF also remarkably declined ($P < 0.05$; Fig. 1F-G). Fig. 1D, H, depicted the typical routes of PNT and SPT, respectively. The findings reveal that NaF impairs learning and memory as well as memory retention capacities in offspring rats.

3.2. NaF exposure induces autophagic flux blockade

To explore the influence of NaF on autophagic flux, we examined the related autophagic indexes by Western blot. Our data suggest that the LC3-II and p62 protein levels of NaF-treated rats were observably enhanced ($P < 0.05$; Fig. 2A-B). Similarly, in SH-SY5Y cells, the tendency was noticed ($P < 0.05$; Fig. 2C-D). To further confirm the effect of NaF-induced autophagic flux, the mRFP-GFP-LC3 adenovirus was used to infect SH-SY5Y cells, which distinguish between autophagosomes and autolysosomes. These results suggest that the number of yellow (autophagosomes) and green fluorescent protein (GFP) puncta was increased, and the number of red puncta (autolysosomes) was decreased after NaF treatment ($P < 0.05$; Fig. 2E-F). In short, these findings indicate that NaF leads to impairment of autophagic substrate degradation, causing autophagic flux blockade.

3.3. NaF exposure induces apoptosis and pyroptosis

To explore the influence of NaF on apoptosis and pyroptosis, we measured the relevant indicators by Western blot. Our findings demonstrated that the cleaved PARP protein level was dramatically elevated in NaF-treated rats ($P < 0.05$; Fig. 3A-B). In SH-SY5Y cells, the result was also concordant ($P < 0.05$; Fig. 3C-D). Furthermore, the NLRP3, Caspase1, and IL-1 β protein levels were observably increased in rats after NaF treatment ($P < 0.05$; Fig. 3E-F). In SH-SY5Y cells, the tendency was consistent ($P < 0.05$; Fig. 3G-H). The results verify that NaF exposure causes apoptosis and pyroptosis in neuronal cells.

3.4. NaF exposure leads to lysosomal number reduced and degradation capacity decreased

To ascertain whether NaF can affect lysosomal biogenesis, we used TEM to observe the change in lysosomal number and Western blot to measure the lysosome-associated proteins. Our findings revealed that the lysosomal number was obviously diminished in the NaF-treated

group (Fig. 4A). As indicated in Fig. 4B, C, in rats, the LAMP2, CTSS, and CTSD protein levels were dramatically decreased when treated with NaF ($P < 0.05$). Consistent with the results in SH-SY5Y cells, the LAMP2, CTSS, and CTSD protein levels were also observably diminished ($P < 0.05$; Fig. 4D-E). Our data reveal that NaF exposure leads to lysosomal biogenesis disorder, as evidenced by the reduction of the lysosomal number and degradation capacity.

3.5. NaF impedes TRPML1/TFEB signaling pathway

The TRPML1/TFEB signaling pathway is critical in regulating lysosomal biogenesis (Tan et al., 2022). Western blot detected to further investigate the association between NaF and lysosomal biogenesis, the expression of the TRPML1/TFEB signaling pathway. In rats treated with NaF, the TRPML1 and nuclear TFEB protein levels were all diminished ($P < 0.05$; Fig. 5A-B). Likewise, in SH-SY5Y cells, the tendency was noticed ($P < 0.05$; Fig. 5C-D). Since TRPML1 is a Ca²⁺ channel located on the lysosomal membrane, its Ca²⁺ release promotes TFEB nuclear translocation, thus promoting lysosomal biogenesis (Medina, 2021). We detected Ca²⁺, LysoTracker, and TFEB nuclear translocation in SH-SY5Y cells by Immunofluorescence assay. The findings indicated that the mean fluorescence intensity of Ca²⁺ and LysoTracker weakened after NaF treatment, which reflected the reduction of Ca²⁺ release and the lysosomal number ($P < 0.05$; Fig. 5E-F). Simultaneously, the TFEB nuclear translocation decreased after NaF treatment ($P < 0.05$; Fig. 5G-H). Furthermore, the TFEB total protein and TFEB cytoplasmic protein levels were also declined after NaF treatment ($P < 0.05$; Fig. S1). Our data demonstrate that NaF exposure inhibits TRPML1 expression and reduces Ca²⁺ release, thereby inhibiting TFEB nuclear translocation.

3.6. TRPML1 activation and TFEB overexpression restore NaF-induced lysosomal biogenesis disorder and dysfunction

After the intervention, we examined the relevant indicators to verify whether TRPML1 activation and TFEB overexpression can restore NaF-induced lysosomal biogenesis and dysfunction. As shown in Fig. 6A-D, ML-SA1 treatment enhanced the nuclear TFEB protein level in the combined treatment group in comparison to the NaF-treated group alone ($P < 0.05$), and a comparable tendency was also noticed when the Ad-TFEB and NaF were treated in combination ($P < 0.05$). In addition, LAMP2 and CTSS protein levels were significantly raised with the combination of ML-SA1 and NaF in comparison to NaF alone treatment ($P < 0.05$; Fig. 6E-F). Similarly, Ad-TFEB also increased LAMP2 and CTSS protein levels after NaF treatment ($P < 0.05$; Fig. 6G-H). Our data reveal that TRPML1 activation and TFEB overexpression restore NaF-inhibited lysosomal biogenesis and degradation capacity.

3.7. TRPML1 activation and TFEB overexpression alleviate NaF-induced autophagic flux blockade, apoptosis, and pyroptosis

To demonstrate that TRPML1 activation and TFEB overexpression can alleviate NaF-induced autophagic flux blockade, apoptosis, and pyroptosis by recovering lysosomal biogenesis as well as degradation capacity, we detected the indicators of autophagy, apoptosis, and pyroptosis after the intervention. As depicted in Fig. 7A-B, the data revealed that ML-SA1 remarkably diminished the p62 protein level ($P < 0.05$) and observably raised the LC3-II protein level in the group of combination treatments ($P < 0.05$). As indicated in Fig. 7C-D, Ad-TFEB observably reduced the LC3-II and p62 protein levels in the group of combination treatments in comparison to the NaF-treated group alone ($P < 0.05$). Subsequently, ML-SA1 and Ad-TFEB notably diminished the cleaved PARP and Caspase1 protein levels after NaF treatment ($P < 0.05$; Fig. 7E-H). Our findings show that TRPML1 activation and TFEB overexpression alleviate autophagic flux blockade, apoptosis, and pyroptosis induced by NaF.

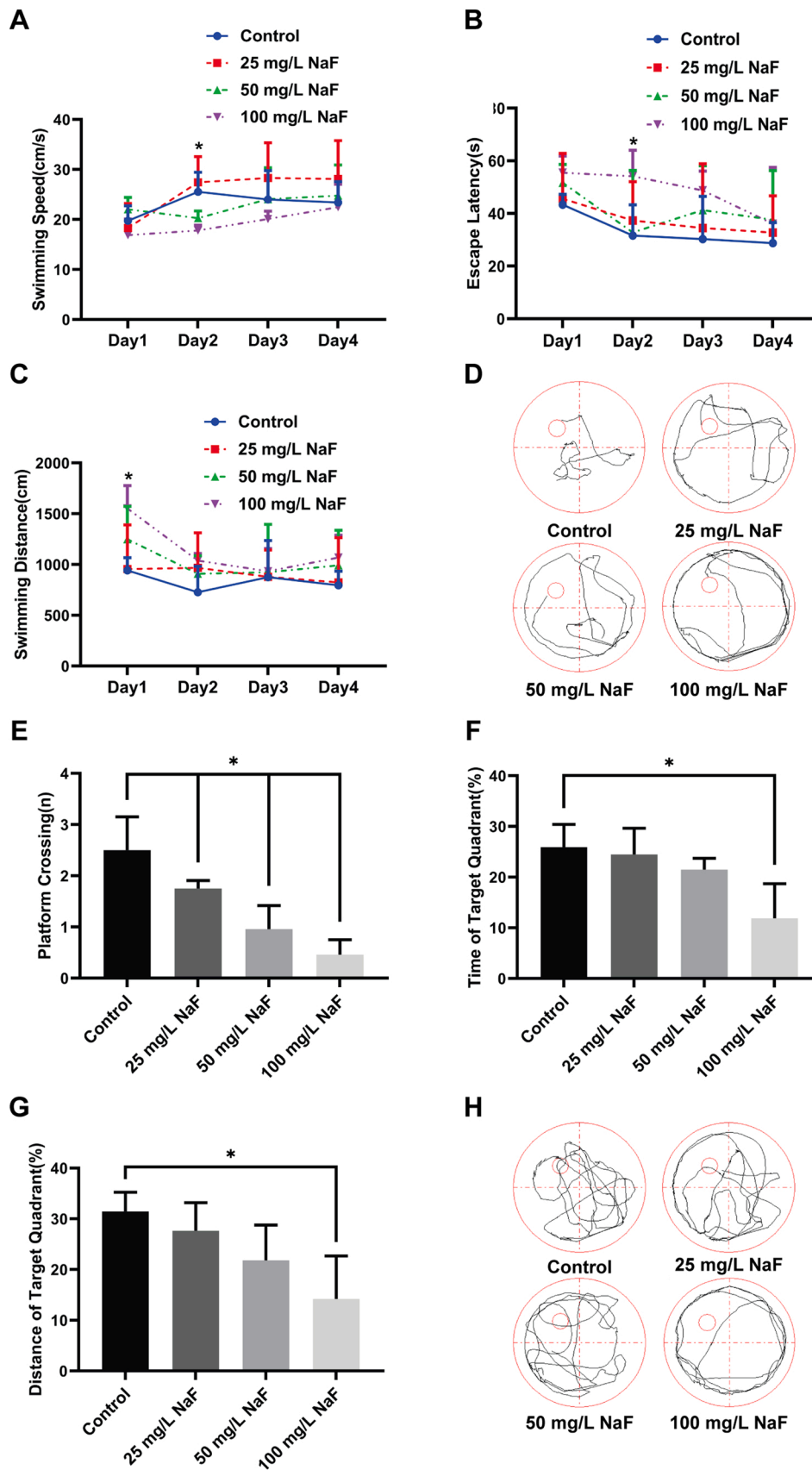


Fig. 1. NaF exposure impairs learning and memory as well as memory retention capacities in offspring rats. (A) The mean swimming speed to the platform. (B) The mean escape latency to the platform. (C) The mean swimming distance to the platform. (D) Representative traces in the PNT. (E) The number of platform crossings. (F) Time spent in the target quadrant. (G) Distance spent in the target quadrant. (H) Representative traces in the SPT. The data are presented for six rats in each group. * $P < 0.05$ versus the control group.

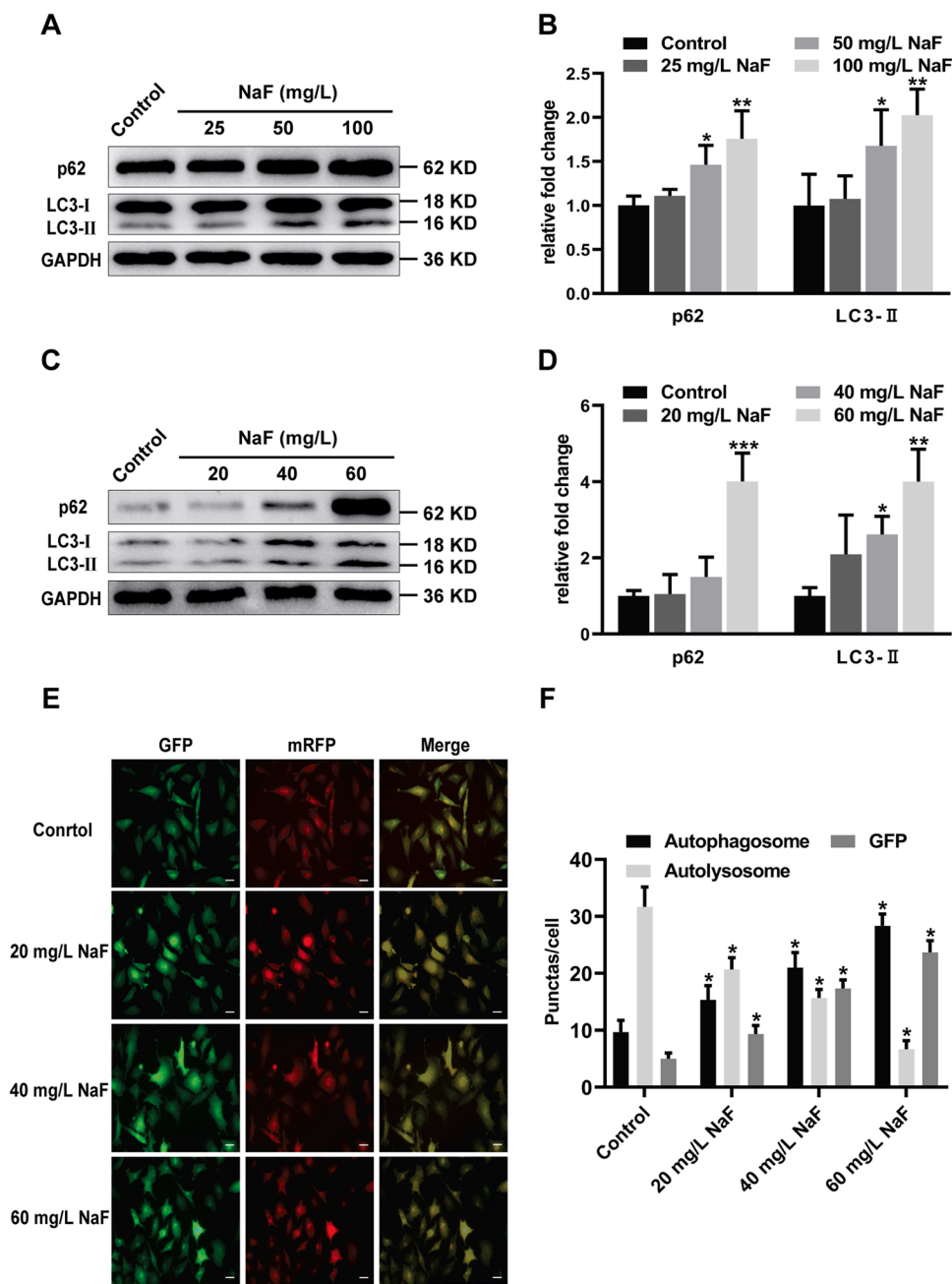


Fig. 2. NaF exposure induces autophagic flux blockade. (A) Representative western blot images for autophagy markers p62 and LC3-II in hippocampal tissues of adult rats. (B) Quantitative analyses of the autophagy markers p62 and LC3-II in hippocampal tissues of adult rats. (C) Representative western blot images for autophagy markers p62 and LC3-II in SH-SY5Y cells. (D) Quantitative analyses of the autophagy markers p62 and LC3-II in SH-SY5Y cells. (E) SH-SY5Y cells were transfected by an mRFP-GFP-LC3 adenovirus and followed by NaF treatment. (F) Quantification of autophagosomes, autolysosomes, and GFP in E. The data are presented as the means \pm S.D. for three different experiments. The scale bar represents 20 μ m. * P < 0.05 versus the control group. ** P < 0.01 versus the control group. *** P < 0.001 versus the control group.

4. Discussion

This study demonstrated that lysosomal biogenesis disorder is a significant cause of developmental fluoride neurotoxicity. Noticeably, NaF inhibited Ca^{2+} release by reducing TRPML1 levels, thereby inhibiting TFEB nuclear translocation and lysosomal biogenesis, leading to decreased lysosomal degradation capacity and autophagic flux blockade and ultimately, developmental fluoride neurotoxicity.

Fluoride has been implicated in several definitive studies as a developmental neurotoxicant (Choi et al., 2015; Jiang et al., 2014). Using a rat model of developmental neurotoxicity, we demonstrated that fluoride exposure during the vital fetal period of neurological development impaired learning and memory as well as memory retention capacities in the offspring. The current findings are consistent with those reported by Chen et al. (Chen et al., 2018), who reported that excessive NaF exposure during pregnancy led to an increase in escape latency and swimming distance, but a decrease in the time and distance spent in the

target quadrants by the rat offspring. Intriguingly, these results are in accordance with epidemiological investigations that have shown that children of women with high fluoride exposure during pregnancy have lower IQs and poorer memory and cognitive competence (Goodman et al., 2022; Green et al., 2019). Our results indicate that excessive NaF exposure weakens learning and memory as well as memory retention capacities in rat offspring, indicating that fluoride impairs neurological development; thus, the model of developmental fluoride neurotoxicity in rats was established successfully.

Autophagy is a dynamic process, also referred to as autophagic flux, which degrades and recycles damaged organelles, misfolded and aggregated proteins, and pathogens in lysosomes. It is essential for the development of the nervous system and the maintenance of neuronal homeostasis (Filippone et al., 2022). In the current study, NaF exposure increased the levels of the LC3-II protein, which is located on the autophagosomal membrane and is essential for the formation of autophagosomes (Zhou et al., 2022b). Thus, our findings indicate that NaF

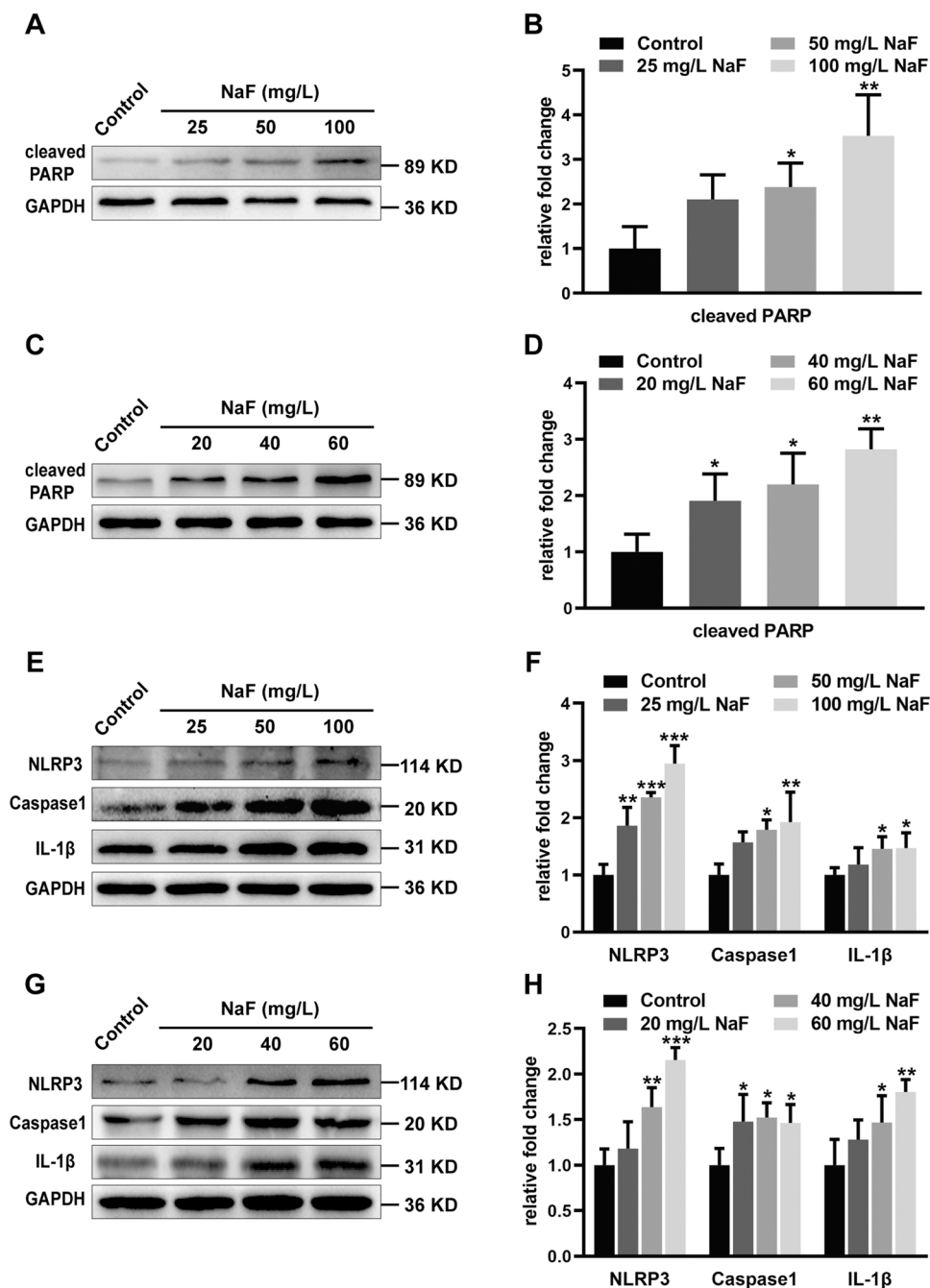


Fig. 3. NaF exposure induces apoptosis and pyroptosis. (A) Representative western blot images for apoptosis marker cleaved PARP in hippocampal tissues of adult rats. (B) Quantitative analyses of the apoptosis marker cleaved PARP in hippocampal tissues of adult rats. (C) Representative western blot images for apoptosis marker cleaved PARP in SH-SY5Y cells. (D) Quantitative analyses of the apoptosis marker cleaved PARP in SH-SY5Y cells. (E) Representative western blot images for pyroptosis markers NLRP3, Caspase1, and IL-1β in hippocampal tissues of adult rats. (F) Quantitative analyses of the pyroptosis markers NLRP3, Caspase1, and IL-1β in hippocampal tissues of adult rats. (G) Representative western blot images for pyroptosis markers NLRP3, Caspase1, and IL-1β in SH-SY5Y cells. (H) Quantitative analyses of the pyroptosis markers NLRP3, Caspase1, and IL-1β in SH-SY5Y cells. The data are presented as the means ± S.D. for three different experiments. **P* < 0.05 versus the control group. ***P* < 0.01 versus the control group. ****P* < 0.001 versus the control group.

induced the accumulation of autophagosomes. Moreover, our data indicated that p62 levels were also increased. As p62 is a selective autophagic receptor, it associates with LC3 and degrades substrates in autolysosomes after autophagosome-lysosome fusion (Zhang et al., 2021a). Hence, enhanced LC3-II and p62 expression is frequently indicative of impaired autophagic degradation. In the present study, in NaF-treated SH-SY5Y cells transfected with mRFP-GFP-LC3, the number of autophagosomes and GFP gradually increased, while the number of autophagolysosomes decreased. The increased GFP levels indicate impaired autophagosome-lysosome fusion. These findings indicate that NaF increased the number of autophagosomes and suppressed autophagosome-lysosome fusion, causing autophagic flux blockade. These findings are in accordance with those of Han et al. (Han et al., 2022), who confirmed that NaF exposure inhibits autophagic degradation and results in autophagic flux blockade, which is probably the

major reason for developmental fluoride neurotoxicity.

Increasing evidence has revealed that autophagic flux blockade leads to apoptosis and pyroptosis (He et al., 2021; Tilija et al., 2022). Apoptosis is a form of programmed cell death. Our results offer compelling evidence in support of neuronal apoptosis induced by NaF, as evidenced by increased levels of cleaved PARP. Recent studies have confirmed that NaF exposure results in defective autophagy, causing apoptosis and inducing neurotoxicity, which is consistent with our findings (Niu et al., 2018). Pyroptosis is an inflammatory programmed cell death characterized by both apoptosis and necrosis. Substantial evidence links pyroptosis with neurodegenerative diseases (Jose et al., 2022; Ma et al., 2022; Nong et al., 2022). In the present study, NaF exposure increased the levels of NLRP3, Caspase1, and IL-1β. NLRP3 is an inflammasome that activates Caspase1 and causes the release of the inflammatory factor IL-1β, leading to pyroptosis (Burdette et al., 2021).

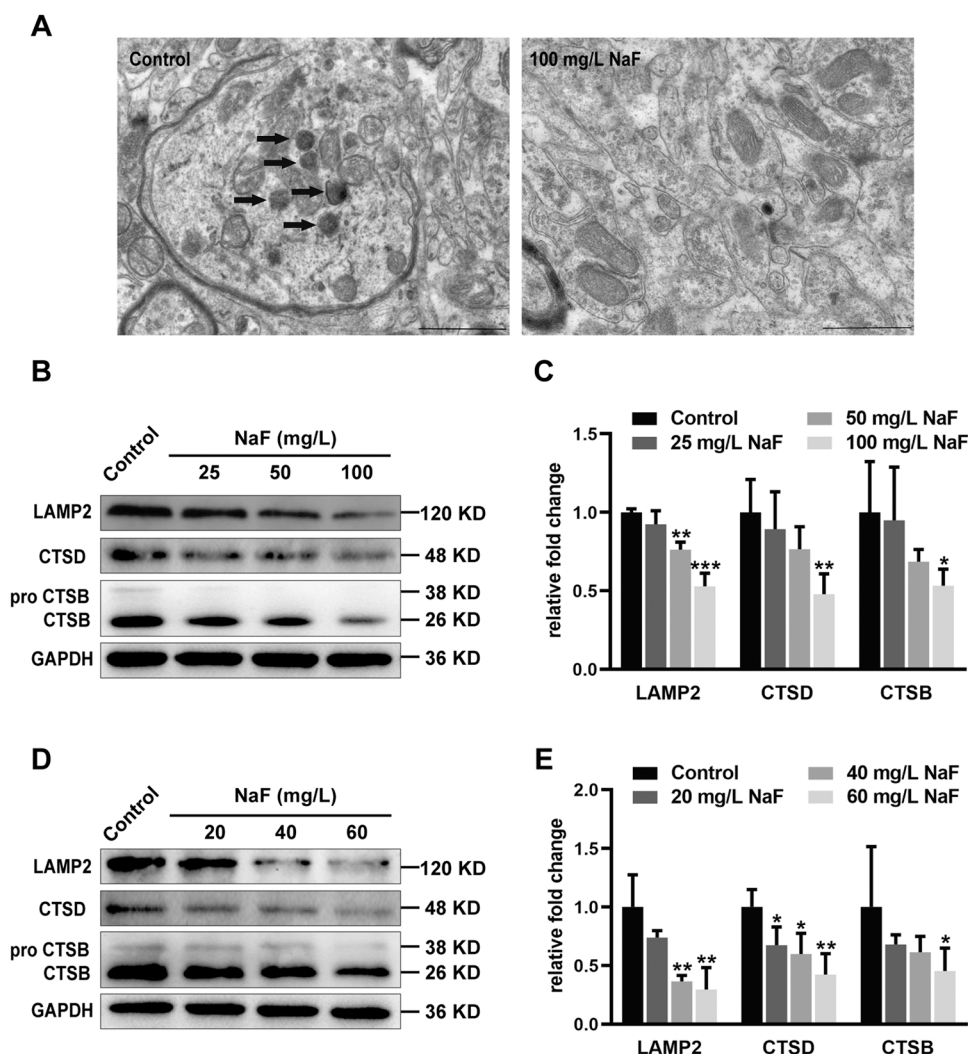


Fig. 4. NaF exposure leads to lysosomal number reduced and degradation capacity decreased. (A) Ultrastructural observation of rat hippocampal region (n = 3). The bold arrow indicates lysosomes. Three rats were randomly selected from each group for evaluation. The scale bar represents 1 μ m. (B) Representative western blot images for lysosomal associated proteins LAMP2, CTSD, and CTSB in hippocampal tissues of adult rats. (C) Quantitative analyses of the lysosomal associated proteins LAMP2, CTSD, and CTSB in hippocampal tissues of adult rats. (D) Representative western blot images for lysosomal associated proteins LAMP2, CTSD, and CTSB in SH-SY5Y cells. (E) Quantitative analyses of the lysosomal associated proteins LAMP2, CTSD, and CTSB in SH-SY5Y cells. The data are presented as the means \pm S.D. for three different experiments. * $P < 0.05$ versus the control group. ** $P < 0.01$ versus the control group. *** $P < 0.001$ versus the control group.

Thus, our data suggest that NaF induces neuronal pyroptosis. Furthermore, our results are consistent with those of a recent study showing that perfluorooctane sulfonic acid (PFOS) exposure activates NLRP3 inflammasomes, resulting in gasdermin D cleavage and IL-1 β release, initiating pyroptosis (Qin et al., 2022). In brief, the current data indicate that apoptosis and pyroptosis induced by NaF cause developmental neurotoxicity.

Lysosomes are the terminal components of autophagic flux, which can degrade and recycle substances in autophagosomes, thus maintaining normal cell function (Banerjee and Kane, 2020). Lysosomal biogenesis is essential for degrading and reusing excess substrates in cells. Notably, we found lysosomal biogenesis disorder after NaF exposure, as evidenced by reduced lysosomal numbers as shown by TEM and decreased LAMP2, CTSD, and CTSB expression. Similar findings were reported by a recent study that NaF exposure caused lysosomal damage, leading to lysosomal dysfunction (Wang et al., 2022). LAMP2 is a prime protein constituent of the lysosomal membrane, which protects the lysosome from the action of hydrolase and maintains the structural integrity of the lysosomal membrane; it is a pivotal factor for lysosomal biogenesis (Eskelinen, 2006). CTSD and CTSB are acidic hydrolases located within lysosomes that are responsible for the degradation of various substrates. The loss of CTSB and CTSD can lead to lysosomal biogenesis disorders and lysosomal dysfunctions, which contribute to various neurological disorders (Drobny et al., 2022). Thus, the above studies indicate that NaF can cause lysosomal biogenesis disorder and reduce the lysosomal degradation capacity of neurons, thus promoting

the progression of fluoride neurotoxicity.

Lysosomal biogenesis and activity are regulated by numerous intracellular and extracellular signals, and the TRPML1/TFEB signaling pathway is crucial for regulating lysosomal biogenesis (Abuammar et al., 2021). As a lysosomal Ca²⁺ release channel, TRPML1 activates calcineurin to translocate dephosphorylated TFEB to the nucleus. Specifically, it recognizes and binds to coordinated lysosomal expression and regulation (CLEAR) elements at the promoters of lysosomal biogenesis-related genes to regulate lysosomal biogenesis (Palmieri et al., 2011). The findings revealed that NaF treatment reduced TRPML1/TFEB expression and Ca²⁺ release, especially TFEB nuclear protein levels, indicating that NaF may inhibit lysosomal biogenesis by decreasing TRPML1/TFEB expression. To further explore the role of the TRPML1/TFEB signaling pathway in developmental neurotoxicity induced by NaF, we added ML-SA1 and Ad-TFEB to NaF-treated SH-SY5Y cells. Our data proved that the upregulation of TRPML1/TFEB increased the TFEB nuclear protein levels and effectively alleviated the NaF-induced decrease in LAMP2 and CTSB expression levels, enhanced lysosomal degradation capacity, and promoted lysosomal biogenesis. These findings were similar to those of Xia et al. (Xia et al., 2020), who identified that ML-SA1 suppresses arboviruses by accelerating lysosomal acidification and proteinase vitality, leading to viral degradation. Cinnamic acid can induce lysosomal biogenesis in primary mouse brain cells by increasing TFEB expression (Chandra et al., 2019). Moreover, alcohol leads to defective autophagy by inhibiting TFEB nuclear translocation, resulting in reduced lysosomal

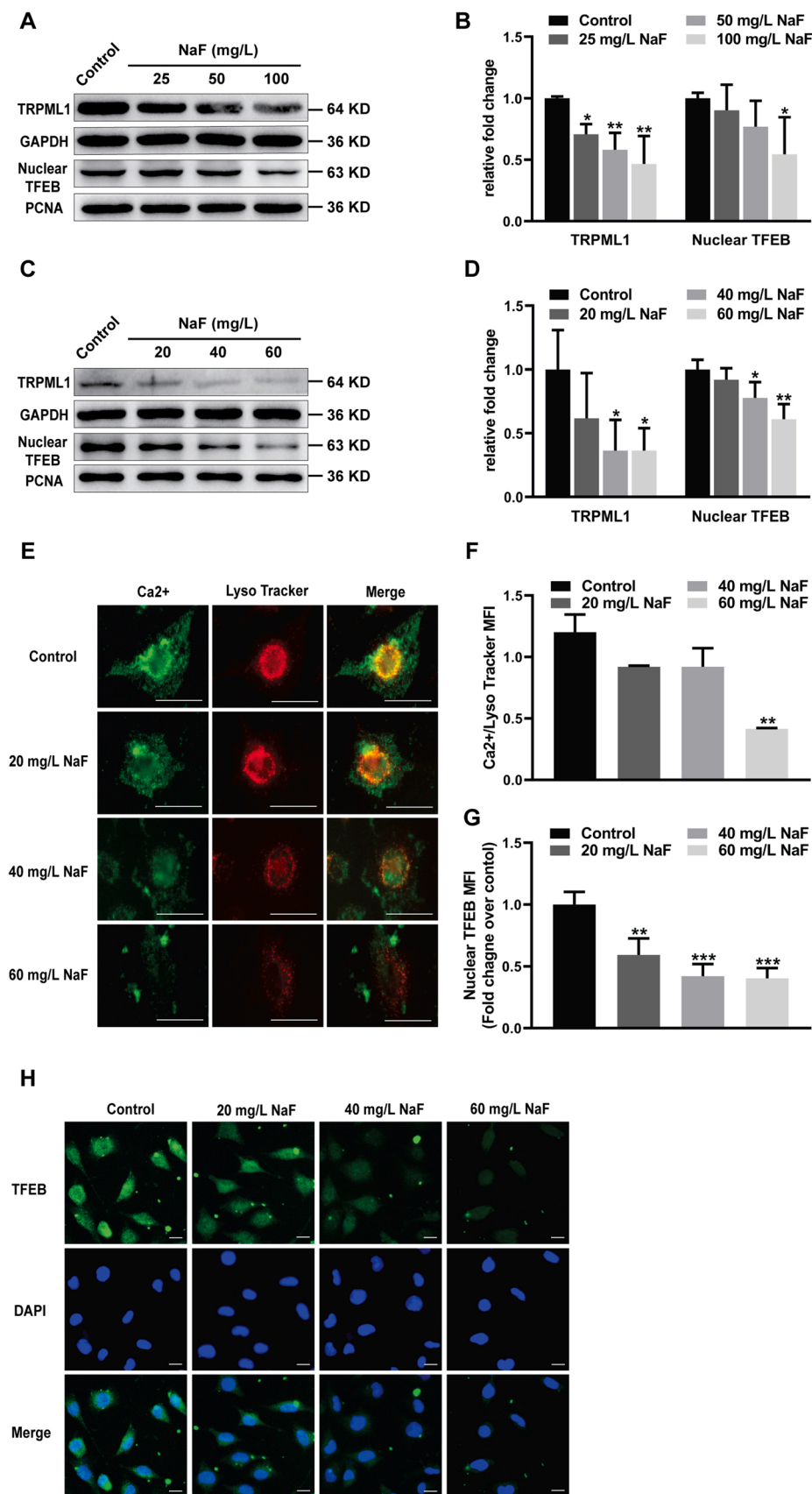


Fig. 5. NaF impedes TRPML1/TFEB signaling pathway. (A) Representative western blot images for TRPML1 and nuclear TFEB in hippocampal tissues of adult rats. (B) Quantitative analyses of TRPML1 and nuclear TFEB in hippocampal tissues of adult rats. (C) Representative western blot images for TRPML1 and nuclear TFEB in SH-SY5Y cells. (D) Quantitative analyses of TRPML1 and nuclear TFEB in SH-SY5Y cells. (E) Representative images of immunofluorescence staining for Ca²⁺ and LysoTracker red in SH-SY5Y cells. (F) Quantitative analyses of E. (G) Quantitative analyses of H. (H) Representative images of immunofluorescent staining ($\times 400$ magnification) for TFEB and DAPI in SH-SY5Y cells. The data are presented as the means \pm S.D. for three different experiments. The scale bar represents 20 μ m. * $P < 0.05$ versus the control group. ** $P < 0.01$ versus the control group. *** $P < 0.001$ versus the control group.

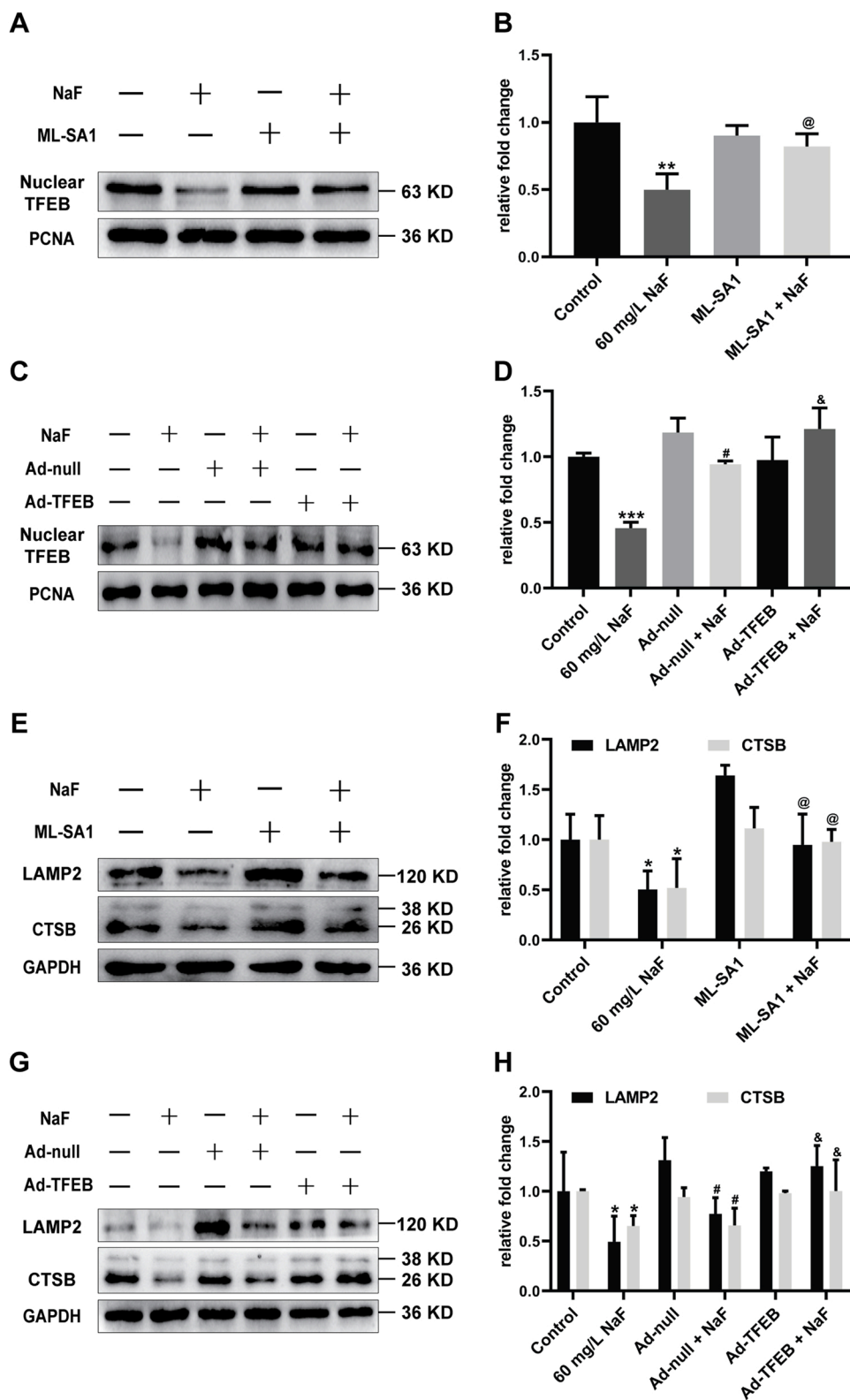


Fig. 6. TRPML1 activation and TFEB over-expression restore NaF-induced lysosomal biogenesis disorder and dysfunction. (A) Representative western blot images for nuclear TFEB in SH-SY5Y cells after NaF combined with ML-SA1 treatment. (B) Quantitative analyses of nuclear TFEB in SH-SY5Y cells. (C) Representative western blot images for nuclear TFEB in SH-SY5Y cells after NaF combined with Ad-TFEB infection. (D) Quantitative analyses of nuclear TFEB in SH-SY5Y cells. (E) Representative western blot images for LAMP2 and CTSB in SH-SY5Y cells after NaF combined with ML-SA1 treatment. (F) Quantitative analyses of LAMP2 and CTSB in SH-SY5Y cells. (G) Representative western blot images for LAMP2 and CTSB in SH-SY5Y cells after NaF combined with Ad-TFEB infection. (H) Quantitative analyses of LAMP2 and CTSB in SH-SY5Y cells. The data are presented as the means \pm S.D. for three different experiments. * $P < 0.05$ versus the control group. ** $P < 0.01$ versus the control group. *** $P < 0.001$ versus the control group. @ $P < 0.05$ versus the NaF treatment group. # $P < 0.05$ versus the Ad-null infection. & $P < 0.05$ versus the combination of Ad-null infection and NaF treatment group.

biosynthesis (Wang et al., 2020). Thus, our results further reveal a pivotal role for TRPML1/TFEB upregulation in promoting lysosomal biogenesis by enhancing the expression of the TFEB nuclear protein.

Interestingly, our findings suggest that TRPML1/TFEB upregulation promotes lysosomal biogenesis while attenuating NaF-induced autophagy flux blockade, thereby reducing apoptosis and pyroptosis. After the ML-SA1 intervention, we found that the expression of the autophagic

degradation substrate p62 and pyroptosis-related Caspase1 was decreased, while levels of LC3-II and cleaved PARP, an apoptosis-related protein, were increased. These findings are similar to those reported by Yan et al. (Yan et al., 2021), who discovered that upregulation of TRPML1 restored autophagic flux, thereby reducing apoptosis. Activation of the adenosine monophosphate-activated protein kinase (AMPK)-TRPML1-calcineurin signaling pathway promotes transcription

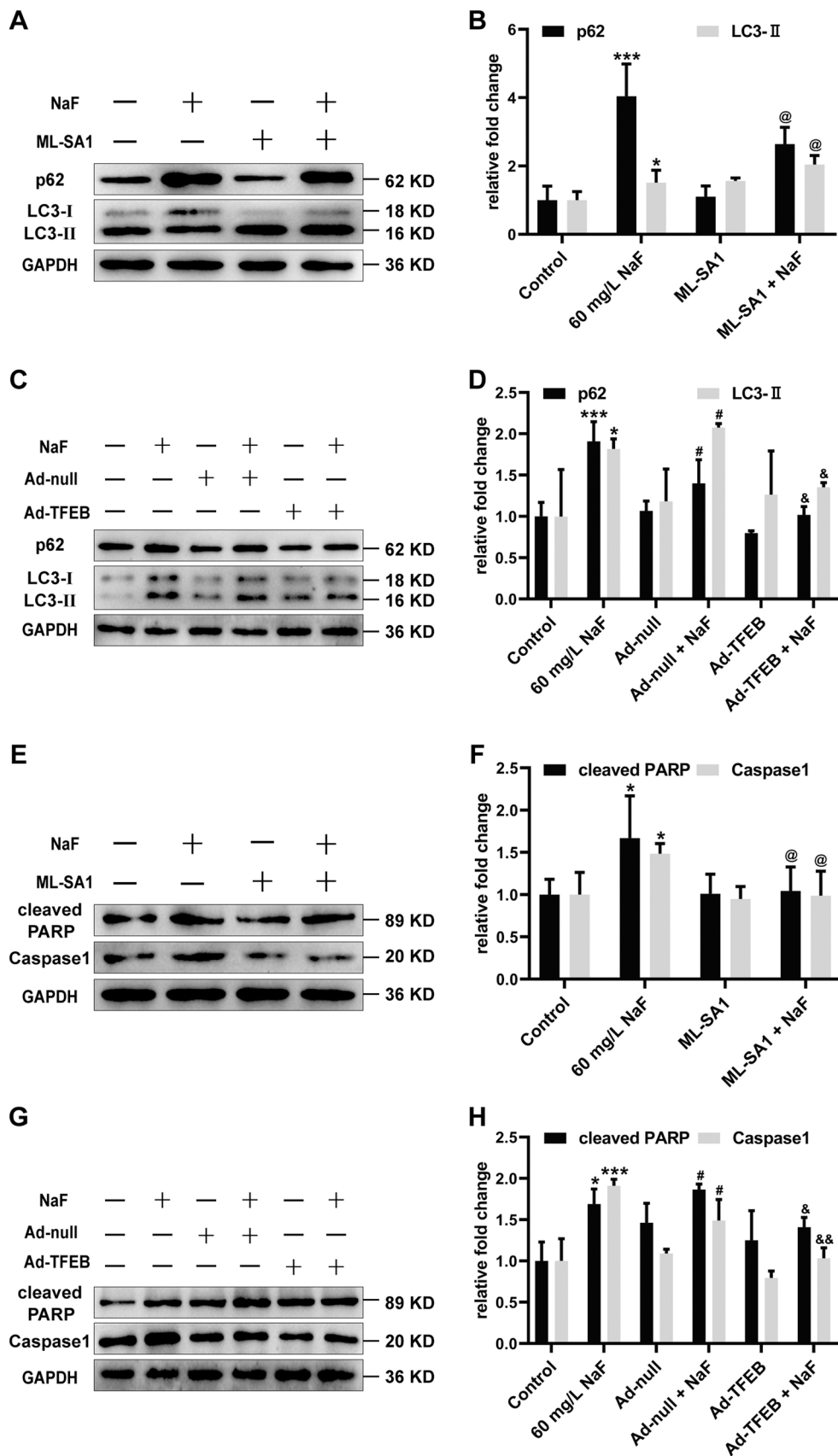


Fig. 7. TRPML1 activation and TFEB over-expression alleviate NaF-induced autophagic flux blockade, apoptosis, and pyroptosis. (A) Representative western blot images for p2 and LC3-II in SH-SY5Y cells after NaF combined with ML-SA1 treatment. (B) Quantitative analyses of p2 and LC3-II in SH-SY5Y cells. (C) Representative western blot images for p2 and LC3-II in SH-SY5Y cells after NaF combined with Ad-TFEB infection. (D) Quantitative analyses of p2 and LC3-II in SH-SY5Y cells. (E) Representative western blot images for cleaved PARP and Caspase1 in SH-SY5Y cells after NaF combined with ML-SA1 treatment. (F) Quantitative analyses of cleaved PARP and Caspase1 in SH-SY5Y cells. (G) Representative western blot images for cleaved PARP and Caspase1 in SH-SY5Y cells after NaF combined with Ad-TFEB infection. (H) Quantitative analyses of cleaved PARP and Caspase1 in SH-SY5Y cells. The data are presented as the means \pm S.D. for three different experiments. * $P < 0.05$ versus the control group. *** $P < 0.001$ versus the control group. @ $P < 0.05$ versus the NaF treatment group. # $P < 0.05$ versus the Ad-null infection. & $P < 0.05$ versus the combination of Ad-null infection and NaF treatment group. && $P < 0.01$ versus the combination of Ad-null infection and NaF treatment group.

factor E3 (TFE3) nuclear translocation, thereby alleviating autophagic flux blockade, thereby attenuating pyroptosis and necrosis (Xu et al., 2021). Similarly, apigenin promotes TFEB nuclear translocation, alleviates lysosomal dysfunction, restores autophagic flux, and suppresses *tert*-butyl hydroperoxide (TBHP)-induced apoptosis of nucleus pulposus cells (Xie et al., 2021). Liraglutide can activate the AMPK-TRPML1-calcineurin signaling pathway, promote TFEB entry into the nucleus and the transcription of autophagy-related proteins, maintain autophagic flux, and reduce pyroptosis (Zhu et al., 2021). These are analogous to our findings. Of note, our results revealed that after Ad-TFEB treatment, the levels of p62, cleaved PARP, Caspase1, and LC3-II were reduced. Since LC3-II is degraded by hydrolases in lysosomes during autophagy (Tanida et al., 2005), if the degradation rate of LC3-II is greater than the formation rate of the autophagosomes, the levels of LC3-II will decrease. Hence, it is possible that Ad-TFEB promotes lysosomal biogenesis and restores lysosomal degradation capacity, thus increasing the rate of lysosomal degradation of LC3-II, which leads to a decline in LC3-II levels. Moreover, as LC3-II levels are variable in different cells, if the background level of autophagy is high in some cells, the LC3-II formed during autophagy activation is rapidly degraded, which can also reduce LC3-II levels. Thus, our findings suggest that TRPML1/TFEB upregulation alleviates autophagic flux blockade induced by NaF, thereby reducing apoptosis and pyroptosis.

5. Conclusion

In summary, we demonstrate that NaF exposure results in lysosomal biogenesis disorder through the inhibition of the TRPML1/TFEB signaling pathway, which leads to autophagic flux blockade, apoptosis, and pyroptosis. Conversely, upregulating TRPML1/TFEB promotes lysosomal biogenesis, enhances lysosomal degradation, maintains autophagic flux, reduces neuronal apoptosis and pyroptosis, and attenuates developmental fluoride neurotoxicity. Our results provide a new therapeutic target for reducing developmental fluoride neurotoxicity. The detailed molecular mechanism of how TRPML1/TFEB signaling promotes lysosomal biogenesis provides a theoretical foundation for the prevention and control of developmental fluoride neurotoxicity.

Funding

This study was supported by funding from the National Natural Science Foundation of China (Grant Nos. 82060580 and 81860559), as well as the Bingtuan Program of Science and Technology Innovation (Grant No. 2021CB046).

CRediT authorship contribution statement

Jingjing Zhang: Investigation, Formal analysis, Methodology, Writing – original draft. **Yanling Tang:** Writing – review & editing. **Zeyu Hu:** Writing – review & editing. **Wanjing Xu:** Visualization, Investigation. **Yue Ma:** Visualization, Investigation. **Panpan Xu:** Visualization. **Hengrui Xing:** Writing – review & editing. **Qiang Niu:** Writing – review & editing, Resources, Conceptualization, Funding acquisition.

Declaration of Competing Interest

The authors declare that they have no known competing financial interests or personal relationships that could have appeared to influence the work reported in this paper.

Data availability

The data that has been used is confidential.

Appendix A. Supporting information

Supplementary data associated with this article can be found in the online version at [doi:10.1016/j.ecoenv.2023.114511](https://doi.org/10.1016/j.ecoenv.2023.114511).

References

- Abduweli, U.D., et al., 2020. Maternal and fetal exposures to fluoride during mid-gestation among pregnant women in northern California. *Environ. Health* 19, 38. <https://doi.org/10.1186/s12940-020-00581-2>.
- Abuammar, H., et al., 2021. Ion channels and pumps in autophagy: a reciprocal relationship. *Cells* 10. <https://doi.org/10.3390/cells10123537>.
- Adkins, E.A., Brunst, K.J., 2021. Impacts of fluoride neurotoxicity and mitochondrial dysfunction on cognition and mental health: a literature review. *Int. J. Environ. Res. Public Health* 18. <https://doi.org/10.3390/ijerph182412884>.
- Angmar-Mansson, B., Whitford, G.M., 1984. Enamel fluorosis related to plasma F levels in the rat. *Caries Res.* 18, 25–32. <https://doi.org/10.1159/000260743>.
2022. Anon, 2022. Guidelines for Drinking-water Quality: Fourth Edition Incorporating the First and Second Addenda, World Health Organization, Geneva.
- Bajaj, L., et al., 2019. Lysosome biogenesis in health and disease. *J. Neurochem.* 148, 573–589. <https://doi.org/10.1111/jnc.14564>.
- Ballabio, A., Bonifacino, J.S., 2020. Lysosomes as dynamic regulators of cell and organismal homeostasis. *Nat. Rev. Mol. Cell Biol.* 21, 101–118. <https://doi.org/10.1038/s41580-019-0185-4>.
- Banerjee, S., Kane, P.M., 2020. Regulation of V-ATPase activity and Organelle pH by phosphatidylinositol phosphate lipids. *Front. Cell Dev. Biol.* 8, 510. <https://doi.org/10.3389/fcell.2020.00510>.
- Burdette, B.E., et al., 2021. Gasdermin D in pyroptosis. *Acta Pharm. Sin. B* 11, 2768–2782. <https://doi.org/10.1016/j.apsb.2021.02.006>.
- Caldas, D.R.D., et al., 2022. Soluble fluoride in Na2FPO3/CaCO3-based toothpaste as an indicator of systemically bioavailable fluoride. *Caries Res.* 56, 55–63. <https://doi.org/10.1159/000521068>.
- Castiblanco-Rubio, G.A., Martínez-Mier, E.A., 2022. Fluoride metabolism in pregnant women: a narrative review of the literature. *Metabolites* 12. <https://doi.org/10.3390/metab12040324>.
- Chandra, S., et al., 2019. Cinnamic acid activates PPARalpha to stimulate Lysosomal biogenesis and lower Amyloid plaque pathology in an Alzheimer's disease mouse model. *Neurobiol. Dis.* 124, 379–395. <https://doi.org/10.1016/j.nbd.2018.12.007>.
- Chen, J., et al., 2018. ERK1/2-mediated disruption of BDNF-TrkB signaling causes synaptic impairment contributing to fluoride-induced developmental neurotoxicity. *Toxicology* 410, 222–230. <https://doi.org/10.1016/j.tox.2018.08.009>.
- Chen, X., et al., 2021. Programmed cell death 4 modulates lysosomal function by inhibiting TFEB translation. *Cell Death Differ.* 28, 1237–1250. <https://doi.org/10.1038/s41418-020-00646-2>.
- Choi, A.L., et al., 2015. Association of lifetime exposure to fluoride and cognitive functions in Chinese children: a pilot study. *Neurotoxicol. Teratol.* 47, 96–101. <https://doi.org/10.1016/j.ntt.2014.11.001>.
- Coelho, P., et al., 2022. Mitochondrial function and dynamics in neural stem cells and neurogenesis: implications for neurodegenerative diseases. *Ageing Res. Rev.* 80, 101667. <https://doi.org/10.1016/j.arr.2022.101667>.
- De Asis-Cruz, J., et al., 2022. Adverse prenatal exposures and fetal brain development: insights from advanced fetal magnetic resonance imaging. *Biol. Psychiatry Cogn. Neurosci. Neuroimaging* 7, 480–490. <https://doi.org/10.1016/j.bpsc.2021.11.009>.
- Dec, K., et al., 2017. The influence of fluorine on the disturbances of homeostasis in the central nervous system. *Biol. Trace Elem. Res.* 177, 224–234. <https://doi.org/10.1007/s12011-016-0871-4>.
- Drobny, A., et al., 2022. The role of lysosomal cathepsins in neurodegeneration: mechanistic insights, diagnostic potential and therapeutic approaches. *Biochim. Biophys. Acta Mol. Cell Res.* 1869, 119243. <https://doi.org/10.1016/j.bbamcr.2022.119243>.
- Eskelinen, E.L., 2006. Roles of LAMP-1 and LAMP-2 in lysosome biogenesis and autophagy. *Mol. Asp. Med.* 27, 495–502. <https://doi.org/10.1016/j.mam.2006.08.005>.
- Ferreira, M., et al., 2021. Fluoride exposure during pregnancy and lactation triggers oxidative stress and molecular changes in hippocampus of offspring rats. *Ecotoxicol. Environ. Saf.* 208, 111437. <https://doi.org/10.1016/j.ecoenv.2020.111437>.
- Filippone, A., et al., 2022. The contribution of altered neuronal autophagy to neurodegeneration. *Pharmacol. Ther.* 238, 108178. <https://doi.org/10.1016/j.pharmthera.2022.108178>.
- Goodman, C.V., et al., 2022. Iodine status modifies the association between fluoride exposure in pregnancy and preschool boys' intelligence. *Nutrients* 14. <https://doi.org/10.3390/nu14142920>.
- Grandjean, P., 2019. Developmental fluoride neurotoxicity: an updated review. *Environ. Health* 18, 110. <https://doi.org/10.1186/s12940-019-0551-x>.
- Green, R., et al., 2019. Association between maternal fluoride exposure during pregnancy and IQ scores in offspring in Canada. *JAMA Pediatr.* 173, 940–948. <https://doi.org/10.1001/jamapediatrics.2019.1729>.
- Gu, X., et al., 2019. Pb disrupts autophagic flux through inhibiting the formation and activity of lysosomes in neural cells. *Toxicol. in Vitro* 55, 43–50. <https://doi.org/10.1016/j.tiv.2018.11.010>.
- Han, X., et al., 2022. Impaired V-ATPase leads to increased lysosomal pH, results in disrupted lysosomal degradation and autophagic flux blockade, contributes to fluoride-induced developmental neurotoxicity. *Ecotoxicol. Environ. Saf.* 236, 113500. <https://doi.org/10.1016/j.ecoenv.2022.113500>.

- He, Y.F., et al., 2021. Lipopolysaccharide induces pyroptosis through regulation of autophagy in cardiomyocytes. *Cardiovasc. Diagn. Ther.* 11, 1025–1035. <https://doi.org/10.21037/cdt-21-293>.
- Jiang, C., et al., 2014. Low glucose utilization and neurodegenerative changes caused by sodium fluoride exposure in rat's developmental brain. *Neuromol. Med.* 16, 94–105. <https://doi.org/10.1007/s12017-013-8260-z>.
- Jose, S., et al., 2022. Mechanisms of NLRP3 activation and pathology during neurodegeneration. *Int. J. Biochem. Cell Biol.* 151, 106273 <https://doi.org/10.1016/j.biocel.2022.106273>.
- Kim, H.K., et al., 2021. TMBIM6 (transmembrane BAX inhibitor motif containing 6) enhances autophagy through regulation of lysosomal calcium. *Autophagy* 17, 761–778. <https://doi.org/10.1080/15548627.2020.1732161>.
- Li, I.H., et al., 2020. Lysosomal dysfunction and autophagy blockade contribute to MDMA-induced neurotoxicity in SH-SY5Y neuroblastoma cells. *Chem. Res. Toxicol.* 33, 903–914. <https://doi.org/10.1021/acs.chemrestox.9b00437>.
- Lou, G., et al., 2020. Mitophagy and neuroprotection. *Trends Mol. Med.* 26, 8–20. <https://doi.org/10.1016/j.molmed.2019.07.002>.
- Ma, X., et al., 2022. Prussian Blue nanozyme as a pyroptosis inhibitor alleviates neurodegeneration. *Adv. Mater.* 34, e2106723 <https://doi.org/10.1002/adma.202106723>.
- Martini-Stoica, H., et al., 2016. The autophagy-lysosomal pathway in neurodegeneration: A TFEB perspective. *Trends Neurosci.* 39, 221–234. <https://doi.org/10.1016/j.tins.2016.02.002>.
- Medina, D.L., 2021. Lysosomal calcium and autophagy. *Int. Rev. Cell Mol. Biol.* 362, 141–170. <https://doi.org/10.1016/bs.ircmb.2021.03.002>.
- Mizushima, N., Levine, B., 2020. Autophagy in human diseases. *N. Engl. J. Med.* 383, 1564–1576. <https://doi.org/10.1056/NEJMr2022774>.
- Mullins, C., Bonifacino, J.S., 2001. The molecular machinery for lysosome biogenesis. *Bioessays* 23, 333–343. <https://doi.org/10.1002/bies.1048>.
- Nagendra, A.H., et al., 2021. Recent advances in cellular effects of fluoride: an update on its signalling pathway and targeted therapeutic approaches. *Mol. Biol. Rep.* 48, 5661–5673. <https://doi.org/10.1007/s11033-021-06523-6>.
- Niu, Q., et al., 2018. Excessive ER stress and the resulting autophagic flux dysfunction contribute to fluoride-induced neurotoxicity. *Environ. Pollut.* 233, 889–899. <https://doi.org/10.1016/j.envpol.2017.09.015>.
- Nong, W., et al., 2022. miR-212-3p attenuates neuroinflammation of rats with Alzheimer's disease via regulating the SP1/BACE1/NLRP3/Caspase-1 signaling pathway. *Bosn. J. Basic Med. Sci.* 22, 540–552. <https://doi.org/10.17305/bjbm.2021.6723>.
- Palmieri, M., et al., 2011. Characterization of the CLEAR network reveals an integrated control of cellular clearance pathways. *Hum. Mol. Genet.* 20, 3852–3866. <https://doi.org/10.1093/hmg/ddr306>.
- Prabhakar, A., et al., 2021. Effect of endemic fluorosis on cognitive function of school children in Alappuzha District, Kerala: a cross sectional study. *Ann. Indian Acad. Neurol.* 24, 715–720. https://doi.org/10.4103/aian.AIAN_850_20.
- Qin, Y., et al., 2022. PFOS facilitates liver inflammation and steatosis: an involvement of NLRP3 inflammasome-mediated hepatocyte pyroptosis. *J. Appl. Toxicol.* 42, 806–817. <https://doi.org/10.1002/jat.4258>.
- Rebiel, R., et al., 2021. Synaptic function and dysfunction in lysosomal storage diseases. *Front. Cell Neurosci.* 15, 619777 <https://doi.org/10.3389/fncel.2021.619777>.
- Souza-Monteiro, D., et al., 2022. Intrauterine and postnatal exposure to high levels of fluoride is associated with motor impairments, oxidative stress, and morphological damage in the cerebellum of offspring rats. *Int. J. Mol. Sci.* 23 <https://doi.org/10.3390/ijms23158556>.
- Tan, A., et al., 2022. Past, present, and future perspectives of transcription factor EB (TFEB): mechanisms of regulation and association with disease. *Cell Death Differ.* 29, 1433–1449. <https://doi.org/10.1038/s41418-022-01028-6>.
- Tanida, I., et al., 2005. Lysosomal turnover, but not a cellular level, of endogenous LC3 is a marker for autophagy. *Autophagy* 1, 84–91. <https://doi.org/10.4161/auto.1.2.1697>.
- Tilija, P.N., et al., 2022. Pitavastatin induces cancer cell apoptosis by blocking autophagy flux. *Front Pharmacol.* 13, 854506 <https://doi.org/10.3389/fphar.2022.854506>.
- Wang, H., et al., 2022. Fluoride exposure induces lysosomal dysfunction unveiled by an integrated transcriptomic and metabolomic study in bone marrow mesenchymal stem cells. *Ecotoxicol. Environ. Saf.* 239, 113672 <https://doi.org/10.1016/j.ecoenv.2022.113672>.
- Wang, M., et al., 2019. Distribution, health risk assessment, and anthropogenic sources of fluoride in farmland soils in phosphate industrial area, southwest China. *Environ. Pollut.* 249, 423–433. <https://doi.org/10.1016/j.envpol.2019.03.044>.
- Wang, S., et al., 2020. Critical role of TFEB-mediated lysosomal biogenesis in alcohol-induced pancreatitis in mice and humans. *Cell Mol. Gastroenterol. Hepatol.* 10, 59–81. <https://doi.org/10.1016/j.jcmgh.2020.01.008>.
- Wei, M., et al., 2022. Effect of fluoride on cytotoxicity involved in mitochondrial dysfunction: a review of mechanism. *Front. Vet. Sci.* 9, 850771 <https://doi.org/10.3389/fvets.2022.850771>.
- Xia, H., et al., 2019. Autophagy in tumour immunity and therapy. *Nat. Rev. Cancer* 21, 281–297. <https://doi.org/10.1038/s41568-021-00344-2>.
- Xia, Z., et al., 2020. ML-SA1, a selective TRPML agonist, inhibits DENV2 and ZIKV by promoting lysosomal acidification and protease activity. *Antivir. Res.* 182, 104922 <https://doi.org/10.1016/j.antiviral.2020.104922>.
- Xie, C., et al., 2021. Apigenin alleviates intervertebral disc degeneration via restoring autophagy flux in nucleus pulposus cells. *Front. Cell Dev. Biol.* 9, 787278 <https://doi.org/10.3389/fcell.2021.787278>.
- Xu, Y., et al., 2021. GDF-11 protects the traumatically injured spinal cord by suppressing pyroptosis and Necroptosis via TFEB-mediated autophagy augmentation. *Oxid. Med. Cell. Longev.* 2021, 8186877. <https://doi.org/10.1155/2021/8186877>.
- Yan, Y., et al., 2021. TRPML1 inhibited photoreceptor apoptosis and protected the retina by activation of autophagy in experimental retinal detachment. *Ophthalmic Res.* 64, 587–594. <https://doi.org/10.1159/000512104>.
- Zhang, W., et al., 2021a. Novel target for treating Alzheimer's Diseases: crosstalk between the Nrf2 pathway and autophagy. *Ageing Res. Rev.* 65, 101207 <https://doi.org/10.1016/j.arr.2020.101207>.
- Zhang, Y., et al., 2021b. Weakened interaction of ATG14 and the SNARE complex blocks autophagosome-lysosome fusion contributes to fluoride-induced developmental neurotoxicity. *Ecotoxicol. Environ. Saf.* 230, 113108 <https://doi.org/10.1016/j.ecoenv.2021.113108>.
- Zhao, Q., et al., 2019. Roles of mitochondrial fission inhibition in developmental fluoride neurotoxicity: mechanisms of action in vitro and associations with cognition in rats and children. *Arch. Toxicol.* 93, 709–726. <https://doi.org/10.1007/s00204-019-02390-0>.
- Zhao, Q., et al., 2020. SIRT1-dependent mitochondrial biogenesis supports therapeutic effects of resveratrol against neurodevelopmental damage by fluoride. *Theranostics* 10, 4822–4838. <https://doi.org/10.7150/thno.42387>.
- Zhao, Y.G., et al., 2021. Machinery, regulation and pathophysiological implications of autophagosome maturation. *Nat. Rev. Mol. Cell Biol.* 22, 733–750. <https://doi.org/10.1038/s41580-021-00392-4>.
- Zhou, J., et al., 2022a. Necessity to pay attention to the effects of low fluoride on human health: an overview of skeletal and non-skeletal damages in epidemiologic investigations and laboratory studies. *Biol. Trace Elem. Res.* <https://doi.org/10.1007/s12011-022-03302-7>.
- Zhou, Y., et al., 2022b. Membrane dynamics of ATG4B and LC3 in autophagosome formation. *J. Mol. Cell Biol.* 13, 853–863. <https://doi.org/10.1093/jmcb/mjab059>.
- Zhu, X., et al., 2021. Liraglutide, a TFEB-mediated autophagy agonist, promotes the viability of random-pattern skin flaps. *Oxid. Med. Cell. Longev.* 2021, 6610603. <https://doi.org/10.1155/2021/6610603>.